Dalton Transactions

Accepted Manuscript

ROYAL SOCIETY OF CHEMISTRY

www.rsc.org/dalton

View Article Online
DOI: 10.1039/C4DT03174A

Vanadyl cationic complexes as catalysts in olefin oxidation

Carla D. Nunes,[a] Pedro D. Vaz,[a,1] Vítor Félix,[b] Luis F. Veiros,[c] Tânia Moniz,[e] Maria Rangel,[d] Sara Realista, [a] Ana C. Mourato,[a] Maria José Calhorda[a]

[a]Centro de Química e Bioquímica, DQB, Faculdade de Ciências, Universidade de Lisboa, 1749−016 Lisboa, Portugal

[b]Departamento de Química, CICECO, Universidade de Aveiro, 3810−193 Aveiro, Portugal

[c] Centro de Química Estrutural, Departamento de Engenharia Química, Instituto Superior Técnico, Universidade de Lisboa , Av. Rovisco Pais, 1049−001 Lisboa, Portugal

[d] *REQUIMTE*, Departamento de Química e Bioquímica, Faculdade de Ciências, Universidade do Porto, 4169-007 Porto, Portugal

[e] *REQUIMTE*, Instituto de Ciências Biomédicas de Abel Salazar, Universidade do Porto, 4099-003 Porto, Portugal

Abstract

Three new mononuclear oxovanadium(IV) complexes [VO(acac)(R−BIAN)]Cl (BIAN = 1,2−bis{(R−phenyl)imino}acenaphthene, R = H, **1**; CH_3, **2**; Cl, **3**) were prepared and characterized. They promoted the catalytic oxidation of olefins such as cyclohexene, *cis*-cyclooctene, and styrene with both tbhp (*tert*-butylhydroperoxide) and H_2O_2, and of enantiopure olefins (*S*(−)− and *R*(+)−pinene, and *S*(−)− and *R*(+)−limonene) selectively to their epoxides, with tbhp as oxidant. Particularly good are the TOFs for styrene epoxidation promoted by complex **3** with H_2O_2 (290 mol mol^{-1}_V h^{-1}) and for *cis*-cyclooctene epoxidation by **2** with tbhp (248 mol mol^{-1}_V h^{-1}). Conversions reached 90% for several systems with tbhp, and were lower with H_2O_2. A preference for the internal C=C bond, rather than the terminal one, was found for limonene. Kinetic data indicate an associative process as the first step of the reaction and complex $[VO(acac)(H-BIAN)]^+$ ($\mathbf{1}^+$) was isolated in a FTICR cell after adding tbhp to **1**. EPR studies provide evidence for the presence of a V(IV) species in solution, until at least 48 hours after the addition of tbhp and *cis*-cyclooctene, and cyclic voltammetry studies revealed an oxidation potential above 1 V for complex **1**. DFT calculations suggest that a $[VO(H-BIAN)(MeOO)]^+$ complex is a likely active V(IV) species in the catalytic cycle from which two competitive mechanisms for the reaction proceed, an *outer sphere*

[1] Present address: ISIS Facility, Rutherford Appleton Laboratory, Chilton, Didcot, Oxfordshire X11 0QX, United Kingdom

View Article Online
DOI: 10.1039/C4DT03174A

path with external attack of the olefin at the coordinated peroxide, and an *inner sphere mechanism* starting with a complex with the olefin coordinated to vanadium.

Keywords: Vanadium / Cationic complexes / Epoxidation / EPR / DFT

Introduction

Vanadium is one of the essential elements of living organisms, playing an important role in several biological processes, namely in halide oxidation catalyzed by haloperoxidases, or in nitrogen fixation carried out by vanadium containing nitrogenases.[1] These aspects contributed to a renewed interest in the coordination chemistry of vanadium,[2] only helped by the applications of vanadium complexes in the clinical treatment of diabetes [3] as well as their potential role as catalysts.[4]

The activity of vanadium enzymes in biological oxidation processes led to the development of a rich oxidation chemistry aimed at the synthesis of valuable molecules. Vanadium complexes are usually active in the presence of H_2O_2, a much more environment friendly oxidant than organic peroxides, which generates water as a by-product. Oxovanadium(IV) complexes are easily synthesized from available precursors, such as vanadyl salts or $[VO(acac)_2]$,[5] and their catalytic activity in a plethora of reactions, ranging from the oxidation of alkenes, to the oxidation of other functional groups,[6] has been widely studied in the presence of several oxidants, such as H_2O_2 or alkylhydroperoxides, and including molecular oxygen,[7] in variable experimental conditions. The immobilization of vanadium species in solids has also led to establishing new active heterogeneous catalysts.[8]

Although VO(IV) complexes are relatively stable toward oxidation, they may be easily oxidized to V(V) in the presence of oxidants. Therefore, when trying to understand the mechanisms of the catalytic reactions promoted by oxovanadium(IV) complexes, a major question concerns the nature of the active catalytic species, in particular the formal oxidation state of vanadium. On the other hand, it is accepted that the mechanism strongly depends on the oxidant, with, for instance, H_2O_2 leading to the formation of peroxide complexes, while in the presence of alkylhydroperoxides (ROOH) the ROO^- anion coordinates to the metal.[9] The role of these complexes has been well described in the oxidation chemistry promoted by molybdenum species, either Mo(VI) complexes, or oxidation products of Mo(II) precursors.[10] Several works have addressed these mechanistic aspects during the last decade,[8,11] but many questions remain open. While it is clear that at the end of the catalysis V(V) species, often catalytically inactive, are present, it is not yet obvious whether the active species is a VO(IV) complex resulting from the reaction of the precursor with the oxidant, without oxidation of the metal. In a systematic mechanistic study,[12] all the likely species

View Article Online
DOI: 10.1039/C4DT03174A

that might be obtained from $[VO(acac)_2]$ and tbhp were calculated (DFT) and their relative energies examined, in order to infer the most pausible mechanism. The possibility of V(IV) active species in catalysis was not discarded and the authors detected their presence in the complex solution in the initial stages of its reaction with tbhp.

In this work, new mononuclear oxovanadium(IV) complexes [VO(acac)(R−BIAN)]Cl (BIAN = 1,2−bis{(R−phenyl)imino}acenaphthene, R = H, CH_3, Cl) have been prepared and characterized by FTIR, ^1H and ^{13}C NMR, and elemental analysis. They were tested for their activity as catalyst precursors in the epoxidation of olefins (*cis*-cyclooctene, ciclohexene, and styrene) and chiral olefins [*S*(−)− and *R*(+)−pinene, and *S*(−)− and *R*(+)−limonene], in the presence of *t*-butylhydroperoxide (tbhp) or H_2O_2 as oxygen sources. Kinetic, EPR, cyclic voltammetry, High Resolution Mass Spectrometry and DFT studies were performed to address the nature of the active catalytic species and the reaction mechanism.

Results and Discussion

Chemical studies

The three bidentate dinitrogen ligands 1,2−bis[(phenyl)imino]acenaphthene (H−BIAN, **L1**), 1,2-bis[(4−methylphenyl)imino]acenaphthene (Me−BIAN, **L2**), and 1,2−bis[(4−chlorophenyl)imino]acenaphthene (Cl−BIAN, **L3**), were prepared according to Scheme 1 and characterized by comparison with literature.[13]

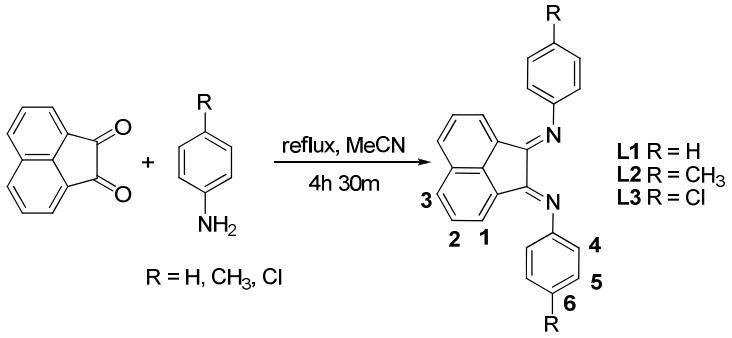

Scheme 1

L1, **L2**, and **L3** were allowed to react with a solution of $[VO(acac)_2]$ in MeOH at reflux, in a 1:1 ratio, to afford complexes [VO(acac)(R−BIAN)]Cl (R-BIAN=**L1**, **1**; L=**L2**, **2**; L=**L3**, **3**), as crystalline powders (Scheme 2). The formulation proposed is based on spectroscopic data and elemental analysis (see Experimental). The molar conductivity of complexes **1-3** (~14.6 S cm^2 mol^{-1}) is lower than the typical for 1:1 salts,[14] though ~5 times higher than that of the $[VO(acac)_2]$

View Article Online
DOI: 10.1039/C4DT03174A

precursor (Λ_m= 2.85 S cm^2 mol^{-1}). This suggests that the chloride is not coordinated to the metal, forming an ion-pair in solution.

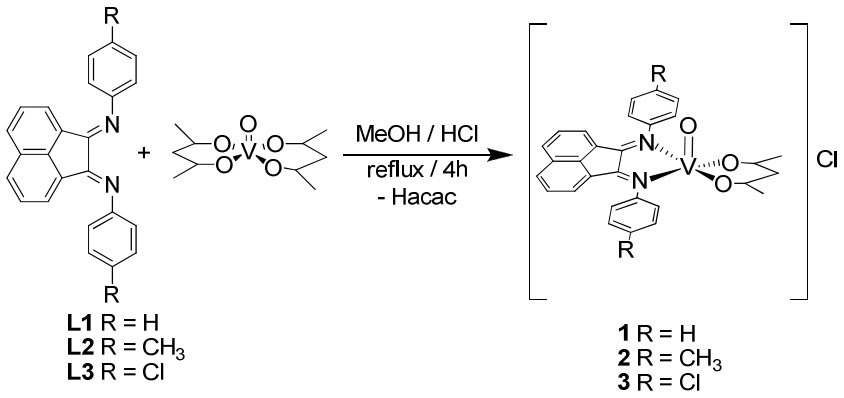

Scheme 2

The coordination of the nitrogen ligands was reflected in the shift of the characteristic $\nu_{C=N}$ vibrational mode in the FTIR spectra, from 1653, 1657, and 1658 cm^{-1}, respectively, in the free ligands L**1**, L**2** and L**3**, to a strong band at 1566, 1560, and 1566 cm^{-1} in the three complexes. The bands observed at 1524, 1523, and 1524 cm^{-1}, for **1**, **2**, and **3**, respectively, are assigned to the C=O, and those at 1486, 1502, and 1485 cm^{-1}, to the C=C stretches of the coordinated acetylacetonate ligand.[15] The strong $\nu_{V=O}$ stretching mode appears as a strong band at 997, 995, and 978 cm^{-1}, for **1**, **2**, and **3**, in agreement with the V=O stretching frequencies reported for other oxovanadium (IV) complexes.[16,17] In the [VO(acac)$_2$] precursor complex this mode is observed at 995 cm^{-1}, suggesting that this strong bond is not much affected by the other ligands around vanadium.

The signals of all the protons of the BIAN and acac ligands could be assigned in the ^{1}H NMR spectra (Experimental, see atom numbering in Scheme 1) of the vanadyl complexes despite the paramagnetism.

The electronic spectra of the ligands **L1**−**L3** present strong absorption at 304 nm, while those of the complexes are observed at 302, 305 or 306 nm for **1**, **2**, and **3**, respectively.

In an attempt to grow crystals of complex **2**, crystals suitable for an X−ray single crystal analysis were obtained by diffusion of a solution of diethyl ether in a solution of methanol. However, they turned out to be the imide of naphthalene-1,8-dicarboxylic acid (**4**) shown in Supplementary Information.

Catalytic studies

The catalytic activity of the three vanadyl complexes [VO(acac)(R−BIAN)]Cl (R= H, **1**; CH$_3$, **2**; Cl **3**) in olefin oxidation was tested in the presence of hydrogen peroxide (H_2O_2) and *t*−

View Article Online
DOI: 10.1039/C4DT03174A

butylhydroperoxide (tbhp), using cyclohexene (Cy6), *cis*-cyclooctene (Cy8), and styrene (Sty), and in the presence of tbhp using the chiral olefins, *S*(−)− and *R*(+)−pinene, and *S*(−)− and *R*(+)−limonene. Control experiments showed that no reaction took place in the absence of a vanadium complex. Detection and identification of products was done by both GC and ^{1}H-NMR experiments. The reaction of complexes **1**−**3** with cyclohexene, *cis*-cyclooctene and styrene was carried out at 328 K using tbhp and H_2O_2 as oxidants (molar ratio of substrate:oxidant:catalyst = 100:200:1), and yielded the corresponding epoxides as the only products. The solvent was dichloromethane with tbhp, and acetonitrile with hydrogen peroxide. This last choice was prompted by the need to avoid a biphasic system, as water started to form after loss of oxygen from H_2O_2, and no epoxide was obtained when dichloromethane was used. The turnover frequencies (TOF) and the conversions of the olefins are given in Table 1.

Table 1. Turnover frequencies and conversions in the epoxidation of cyclohexene, *cis*-cyclooctene, and styrene using complexes [VO(acac)(R−BIAN)]Cl (**1**−**3**) as catalyst precursors, and tbhp or H_2O_2 as oxidants, at 328 K.

		tbhp		H_2O_2	
Complex	Olefin	TOF[a]	Conv.[b]	TOF[a]	Conv.[b]
1	Cy6	222	92	254	85
	Cy8	191	82	184	66
	Sty	212	78	264	77
2	Cy6	222	98	210	78
	Cy8	248	93	162	76
	Sty	218	83	286	69
3	Cy6	235	90	252	91
	Cy8	187	87	110	54
	Sty	216	76	290	77

[a] calcd. at 0.25 h as mol mol^{-1}[V] h^{-1}; [b] calcd. after 24 h

The three complexes **1**−**3** exhibit relatively similar initial catalytic activities for all substrates with both oxidants, although there is a smaller dispersion with tbhp, with TOFs ranging between 187 to 248 mol mol$^{-1}_{V}$ h^{-1}; when using H_2O_2 as oxidant, the TOFs can go down to 110 (Cy8) and up to 290 mol mol$^{-1}_{V}$ h^{-1} (Sty).

View Article Online
DOI: 10.1039/C4DT03174A

With tbhp, the highest initial activity in the oxidation of cyclohexene is achieved when complex **3** is the precursor (TOF of 235 mol mol^{-1}_{V} h^{-1}), with small differences from the other complexes, while complex **2** is the best for *cis*-cyclooctene (248 mol mol^{-1}_{V} h^{-1}). All behave similarly toward styrene. Conversions are usually higher with tbhp than with H_2O_2, the highest conversion being achieved in the epoxidation of cyclohexene with any of the catalysts (90−98); complex **2** leads to higher conversions independently of the substrate, and is thus less substrate-selective. When H_2O_2 is used, the trends are less clear and conversions can be as low as 54 (Cy8 with complex **3**). Although H_2O_2 might be considered a more environment friendly oxidant, as it leads to formation of H_2O, the by-product of tbhp (*t*-butanol) has many applications.

The kinetic profiles shown in Figure 1 for the oxidation of Cy6 using both oxidants and the three catalyst precursors give a more detailed view of the reaction pattern. The reaction is initially fast in all cases, reaching a conversion of ~70 % in about one hour, consistent with the formation of the active species after addition of the oxidant, and a plateau after a few hours. It has been shown for Mo(VI) catalysts that the formed *t*-BuOH (or H_2O) competes with the oxidant in the reaction with the metal center, [10,18] thus decreasing the conversion. A similar observation was reported for vanadium catalysts.[6a] The final conversions of Cy6 are very close in the presence of complexes **1** and **3**, but differ more for complex **3** (methyl substituent). The lower conversion in H_2O_2 may be associated with lower solubility of **3**.

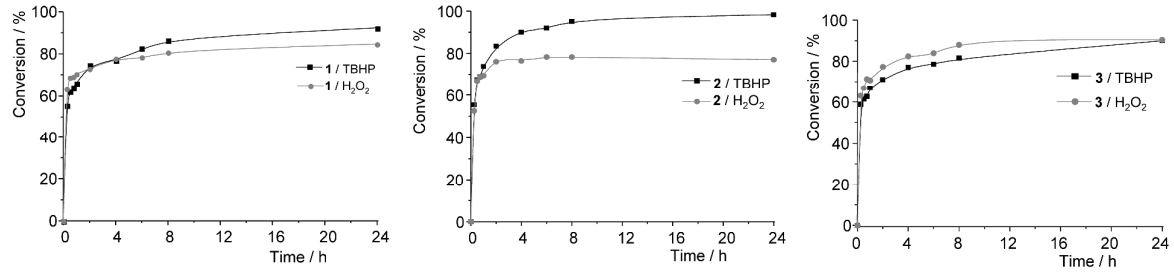

Figure 1. Kinetic profiles for the epoxidation of Cy6 catalyzed by complexes [VO(acac)(**L**)]Cl (**1**−**3**), in the presence of tbhp or H_2O_2 (molar ratio of substrate:oxidant:catalyst = 100:200:1), at 328 K.

View Article Online
DOI: 10.1039/C4DT03174A

As a comparison, [VO(Saloph)] (Saloph = N,N'-disalicylidene-o-phenylenediaminate) converted only 10.7 % of styrene after 2 hours at 363 K with tbhp, though with a higher TOF (726 mol mol^{-1}[V] h^{-1}). [8] VO(Schiff base) containing polymers also exhibited styrene conversions between 12 and 76 % at 348 K (tbhp, 6 hours) depending on substrate:catalyst:oxidant ratios.

The vanadium complexes [VO(acac)(R−BIAN)]Cl (**1**−**3**) were also tested in the catalytic epoxidation of four enantiopure chiral olefins, *S*(−)− and *R*(+)−pinene, and *S*(−)− and *R*(+)−limonene, at 328 K, in dichloromethane, using tbhp as the oxygen source (molar ratio of substrate:oxidant:catalyst = 100:200:1). Only epoxides (Scheme 3) were formed, confirming the high selectivity already observed in the experiments described above. The limonene substrates have two competing olefin sites where epoxidation may occur, but NMR experiments demonstrated that only the epoxides shown in Scheme 3 are formed, indicating that such catalytic systems are chemospecific, and there is retention of configuration.

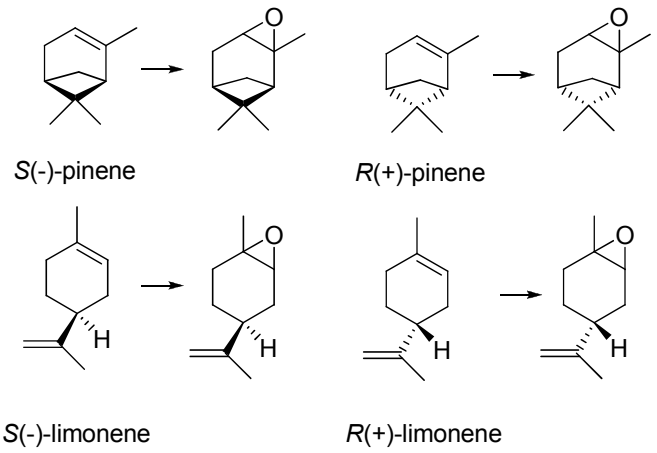

Scheme 3

The initial activities do not follow a specific trend, but vary within narrow intervals (177 to 243 mol·mol$^{-1}_{V}$·h^{-1}), comparable to those found above (Table 1). Complex **2** leads to the highest TOFs with *S*(−) olefins, while complex **3** displays a preference for *R*(+) molecules.

The conversions are found to be above 70%, with a maximum of 87% for the complex **2**/ S(−)−limonene system, again resembling the values obtained for the first set of substrates (Table 1). Although the catalytic systems exhibit a high selectivity (only one epoxide, with retention of configuration), their efficiency in terms of conversion is not outstanding.

View Article Online
DOI: 10.1039/C4DT03174A

Table 2. Turnover frequencies and conversions in the epoxidation of *S*(−) and *R*(+)−pinene, and *S*(−) and *R*(+)−limonene, using complexes [VO(acac)(R−BIAN)]Cl (**1**−**3**) as catalyst precursors, and tbhp as oxidant.

Complex	Olefin	TOF[a]	Conv.[b]
1	*S*(−)−pinene	192	82
	S(−)−limonene	**201**	**87**
	R(+)−pinene	**204**	**83**
	R(+)−limonene	194	81
2	*S*(−)−pinene	**243**	**83**
	S(−)−limonene	**193**	**87**
	R(+)−pinene	198	73
	R(+)−limonene	188	81
3	*S*(−)−pinene	202	82
	S(−)−limonene	177	80
	R(+)−pinene	**208**	**85**
	R(+)−limonene	**223**	**82**

[a] calcd. at 0.25 h as mol mol^{-1}[V] h^{-1}; [b] calcd. after 24 h

UV/Vis and Mass Spectrometry Kinetic Studies

Kinetic studies were carried out in the reaction of complexes [VO(acac)(R−BIAN)]Cl (**1**−**3**) with each of the oxidants (tbhp and H_2O_2) in order to investigate the formation of the catalytically active species, and evaluate the role of the H, CH_3 and Cl ligand−substituents on the metal. Gould et al.[6a] performed a similar study for the epoxidation of cyclohexene catalyzed by [$VO(acac)_2$] and V(III) complexes, after checking the absence of radical pathways.

The disappearance of the initial vanadyl complex was followed by UV/Vis spectroscopy. The kinetics of the formation of the first intermediate shows a first order reaction in metal complex and in oxidant. The observed rate constants were determined by fitting the absorbance *vs* time data to the equation

$$A_t = A_\infty(1 - e^{-k_{obs}t}) - \text{offset} - L * t \quad (1)$$

where A_t and A_∞ are the absorbances at time t and at the end of reaction, respectively, the offset is the absorbance value at t = 0 s, and the L parameter takes into account a very small drift observed in

View Article Online
DOI: 10.1039/C4DT03174A

the absorbance *vs* time data at the end of the reaction.[19] An example of a typical curve is shown in Figure 2, for complex **3** and tbhp, at 303 K, and with a molar ratio 1:100 (complex:tbhp).

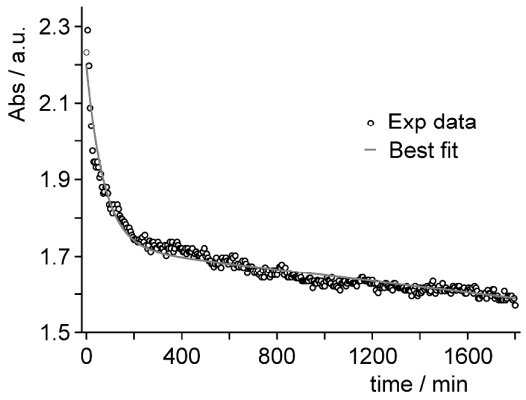

Figure 2. Change in absorbance during the reaction between complex **3** and tbhp at 303 K (experimental points and fit according to equation 1).

The observed pseudo−first order rate constants k_{obs}, calculated varying the concentration of the oxidant and keeping the concentration of the complex (**1**−**3**) constant (1×10^{-4} M) at 298 K, are summarized in Table 3.

Table 3. Kinetic data (k_{obs}) for the reaction between complexes [VO(acac)(R−BIAN)]Cl (**1**−**3**) and at different concentrations of the oxidants (tbhp or H_2O_2), in acetonitrile, at 298 K.

Oxidant	10^3 [Ox] / M	k_{obs} / s^{-1}		
		1	**2**	**3**
tbhp	0.101	2.4 ± 0.2	3.0 ± 0.2	3.1 ± 0.1
	0.202	2.8 ± 0.2	3.7 ± 0.2	4.1 ± 0.1
	0.505	3.8 ± 0.2	8.1 ± 0.2	7.7 ± 0.1
	1.010	7.2 ± 0.2	12.5 ± 0.2	14.5 ± 0.2
H_2O_2	0.101	10.6 ± 0.1	7.5 ± 0.1	10.0 ± 0.1
	0.202	21.3 ± 0.1	11.2 ± 0.1	16.0 ± 0.2
	0.505	33.0 ± 0.1	23.4 ± 0.7	30.4 ± 0.2
	1.010	53.9 ± 0.3	37.2 ± 0.9	54.7 ± 0.3

The fit of k_{obs} values *vs.* oxygen donor concentration was done according to equation $k_{obs}= k_2$[Oxidant], where k_{obs} is the pseudo−first order rate constant and k_2 is the second−order rate constant. The fit shows, in the presence of excess of tbhp or H_2O_2, a clear first-order dependence on

View Article Online
DOI: 10.1039/C4DT03174A

the concentration of the oxidant (tbhp or H_2O_2). The second-order rate constants (k_2) for the reaction of the three complexes [VO(acac)(R−BIAN)]Cl (**1**−**3**) with tbhp at several temperatures are given in Table 4.

Table 4. Second−order rates (k_2) for the reaction between complexes [VO(acac)(R−BIAN)]Cl (**1**−**3**) and the oxidants (tbhp or H_2O_2), in acetonitrile, in the 298−333 K temperature range.

Oxidant	T / K	k_2 / dm^3 mol^{-1} s^{-1}		
		1	**2**	**3**
tbhp	298	5.2 ± 0.1	10.8 ± 0.2	12.6 ± 0.1
	303	9.6 ± 0.2	14.6 ± 0.2	13.5 ± 0.2
	313	16.0 ± 0.4	18.8 ± 0.5	14.7 ± 0.4
	328	23.6 ± 1.8	32.6 ± 1.2	16.9 ± 0.5
	333	33.7 ± 1.8	42.0 ± 0.7	17.6 ± 0.4
H_2O_2	298	45.0 ± 0.2	32.7 ± 0.5	48.7 ± 0.2
	303	56.0 ± 0.3	37.4 ± 0.5	67.4 ± 0.4
	313	93.6 ± 0.2	61.4 ± 0.7	87.2 ± 0.4
	328	143.6 ± 0.4	86.8 ± 0.8	120.8 ± 0.6
	333	165.0 ± 1.0	113.0 ± 2.5	125.1 ± 0.75

The reaction with H_2O_2 is much faster than with tbhp, though the acceleration with increasing temperature is not the same from one oxidant to the other and with different complexes. The activation parameters $\Delta S^{\neq}$ and $\Delta H^{\neq}$ for catalyst formation were determined from the kinetic data (Table 5) obtained in the range of 298–333 K, by fitting the second order rate constants with the Eyring equation:

$$\ln\left(\frac{k_2}{T}\right) = \frac{-\Delta H^{\ddagger}}{R}\cdot\frac{1}{T} + ln\left(\frac{k_B}{h}\right) + \frac{\Delta S^{\ddagger}}{R}$$

where k_2 is the second-order rate constant, T temperature (K), R, k_B and h are the gas, Boltzmann, and Planck constants. $\Delta H^{\neq}$ and $\Delta S^{\neq}$ are the activation enthalpy and entropy, respectively.

The effect of the substituent on the BIAN ligand in the rate constants and activation parameters is clear. When the oxidant is tbhp, rate constants increase in the order **1** < **2** ≈ **3**; when H_2O_2 is used as the oxygen source, the trend is **2** < **1** ≈ **3** (Table 4).

The large and negative $\Delta S^{\neq}$ values indicate an associative mechanism for the first step in the activation of the vanadyl complexes **1**−**3**. The $\Delta H^{\neq}$ values are relatively low in general, with a

View Article Online
DOI: 10.1039/C4DT03174A

minimum for complex **3,** [VO(acac)(Cl−BIAN)]Cl, in the reaction with tbhp. These values are comparable, though lower, than $\Delta H^{\neq} \approx 54$ kJ mol^{-1}obtained in the similar reaction between [$VO(acac)_2$] and tbhp, in the earlier study of Gould et al,[6a] where cyclohexane was used as solvent in the absence of alkene; the $\Delta S^{\neq}$ value was also very negative (–83 J mol^{-1} K^{-1}). Although it is expected that a similar reaction will take place, there are significant differences between [$VO(acac)_2$] and cationic complexes [VO(acac)(Cl−BIAN)]Cl (**1**−**3**) to justify the disparities. More interesting is the comparison with several MoO_2(VI)/tbhp systems for which the calculated activation enthalpies ($\Delta H^{\neq} \approx 50$ kJ mol^{-1}) are much closer.[19] In these systems, there is no oxidation of the metal center, and it is known that the first step consists of the activation of the O−H bond of the alkylhydroperoxide, which protonates one oxide, while the ROO^- anion binds the metal. On the other hand, in the CH_3ReO_3/H_2O_2 system, the activation enthalpy is lower ($\Delta H^{\neq} = 29$ kJ mol^{-1}) and the initial step is not the same (probably peroxide complexes are formed). [20]

Table 5. Activation parameters $\Delta S^{\neq}$ and $\Delta H^{\neq}$ for the reaction between complexes [VO(acac)(R−BIAN)]Cl (**1**−**3**) and the oxidants (tbhp or H_2O_2 in MeCN).

Oxidant	Complex	$\Delta H^{\neq}$ / kJ.mol^{-1}	$\Delta S^{\neq}$ / J.mol^{-1} K^{-1}
tbhp	**1**	36.4 ± 5.2	-107.4 ± 18.1
	2	27.6 ± 1.8	-132.2 ± 19.2
	3	5.1 ± 0.1	-206.6 ± 19.7
H_2O_2	**1**	28.0 ± 1.9	-118.9 ± 19.2
	2	26.0 ± 2.0	-128.8 ± 19.1
	3	18.7 ± 2.5	-149.0 ± 18.9

The mechanism of the reaction between complexes [VO(acac)(R−BIAN)]Cl (**1**−**3**) and tbhp has an associative nature and could start with a bond breaking process, probably the O–H bond in ROOH. The ROO^- ligand may then transfer the oxygen to the alkene substrate, forming epoxide and butanol. The catalytic experiments show the decay in activity associated with formation of the alcohol, which competes with the alkylhydroperoxide to yield the active species, a fact that has been well demonstrated in Mo(VI) systems.[19]

High-resolution mass spectrometry (HRMS) experiments were also carried out to study the formation of vanadium species in the presence of the oxidant (tbhp) and to complement it the detection of the relevant species produced in the reactions, which is possible under MS conditions. The experiments were carried out adopting ESI-MS as the ionization technique and using collision

View Article Online
DOI: 10.1039/C4DT03174A

induced dissociation (CID) on a FTICR spectrometer. This equipment returns the exact masses of the observed fragments, and allows an accurate isolation of a given fragment. This can afterwards react with another reactant introduced by means of an inlet valve. The first experiment was accomplished by mixing complex **1** with tbhp (ratio 1:10) in acetonitrile (conditions similar to those used in the UV/Vis experiments). Analysis of the resulting mixture (after addition of methanol for a good quality spray) evidenced the presence of a single species containing vanadium detected at m/z = 611.24, which can be formulated as $[C_{33}H_{40}N_2O_6V]^+$. This formula corresponds to a species $[VO(H-BIAN)(tbhp)_2(CH_3OH)]^+$, which can easily lose the methanol molecule to yield the complex $[VO(H-BIAN)(tbhp)_2]^+$ (**1x**) detected at m/z = 579.21. This result shows that, in the presence of tbhp, complex **1** loses easily the acac ligand, which is replaced by two tbhp molecules. The species **1x** can be considered as a rest mode of the catalyst prior to reaction with the olefin. To confirm this hypothesis, kinetics were conducted with the MS spectrometer. Complex $[VO(acac)(H-BIAN)]^+$ ($\mathbf{1}^+$, detected at m/z = 498.11) was isolated in the ICR cell and allowed to react with added tbhp with increasing time. The kinetic curve in Figure 3 evidences the reaction of $\mathbf{1}^+$ with tbhp given by the decrease of the peak intensity. In a second experiment, complex **1x** was isolated and made to react with *cis*-cyclooctene to check if this could be the active species. In fact, the decrease of the peak intensity of **1x** with increasing reaction time, though at a slower rate than the first step, supports this idea.

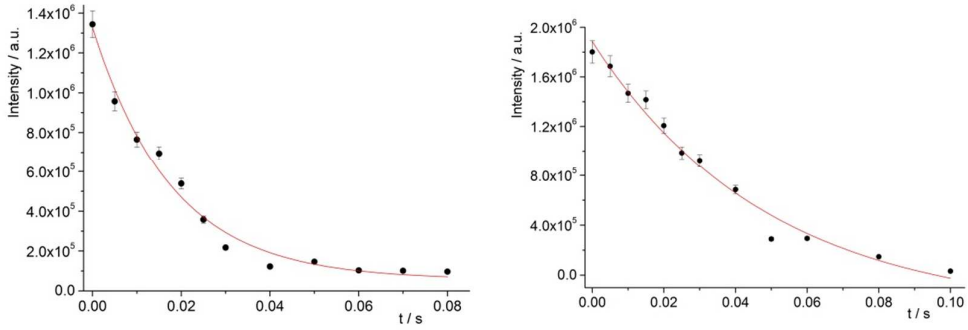

Figure 3. HR-MS kinetic experiments for the reactions: $\mathbf{1}^+$ with tbhp yielding **1x** (left); **1x** with *cis*-cyclooctene (right).

The comparison between the two kinetic experiments shows that the second step can be defined as the rate limiting step, at least in the early stages of the catalytic cycle. These results provide strong evidence that the active species is based on a V(IV) complex, since the proposed V(IV) complexes were observed at the right m/z ratios and no other V species were detected.

View Article Online
DOI: 10.1039/C4DT03174A

EPR studies

The investigation of the oxidation state of the metal in the active catalytic species was carried out by Electron Paramagnetic Resonance, by studying the reaction between the initial complex and tbhp, and the reaction between complex **1**, tbhp and substrate (*cis*-cyclooctene, Cy8).

At room temperature, complex [VO(acac)(H−BIAN)]Cl (**1**) exhibits a well resolved isotropic signal, which exhibits anisotropy upon freezing the solution (Figure 4). The **g** and **A** values are within the expected values for this type of V(IV) d^1 complex and the computer simulation of the experimental spectra reproduces well the observed features and provides the values of the Spin-Hamiltonian parameters.

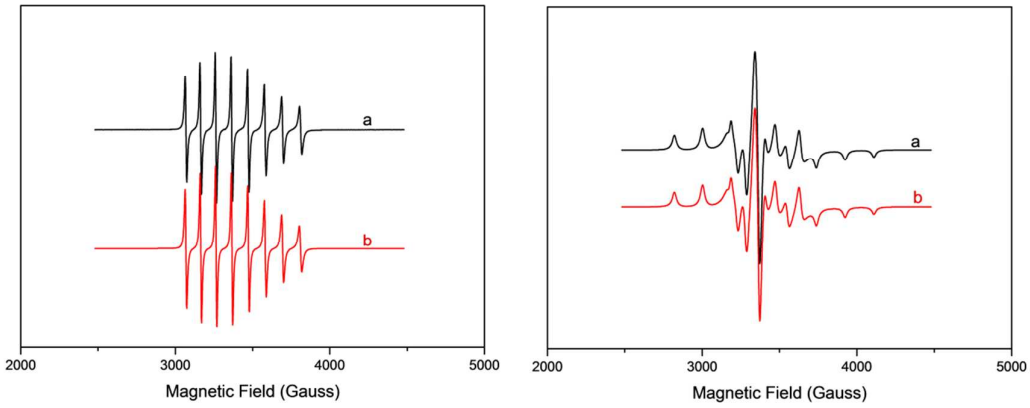

Figure 4. EPR signal of complex [VO(acac)(H−BIAN)]Cl (**1**) obtained in dichloromethane at 296 K (left) and in frozen matrix at 100 K (right). Experimental (a) and simulated (b) spectra. Spin-Hamiltonian parameters obtained by simulation of the EPR spectra of complex **1**: g_{iso} = 1.959, A_{iso}= 97.0 x 10^{-4} cm^{-1} at 296 K and g_1 = 1.9785, A_1= 60.5 x 10^{-4} cm^{-1}; g_2 = 1.9660, A_2= 64.0 x 10^{-4} cm^{-1}; g_3 = 1.9476, A_3= 167.5 x 10^{-4} cm^{-1} at 100 K.

Tbhp was added to a dichloromethane solution of complex **1** and tbhp plus Cy8 were also added to a solution of **1**. Upon addition of the reagents, the EPR signal was not lost and its evolution along time is shown in Figure 5 (see also Figure S3 in Supplementary Information). The signal of complex **1** at 100 K (a) is easily identified by comparison with Figure 4. When tbhp is added, a less intense signal remains (b). It is almost superimposable with (a), and characteristic of a V(IV) complex. The signal obtained after addition of tbhp + Cy8 to complex **1** (c) is practically the same and has not changed after 24 hours (d).These results indicate that despite the large excess of oxidant, as in the catalytic conditions, a V(IV) species remains in solution and is still there 24 hours later. The analysis of the spectra, registered along time, is indicative of the presence of the V(IV) species and of a variation of the intensity of the signals, which is consistent with a variation in

View Article Online
DOI: 10.1039/C4DT03174A

concentration of the paramagnetic species. These experiments prove the presence of a V(IV) species in solution under catalytic conditions for at least 24 hours.

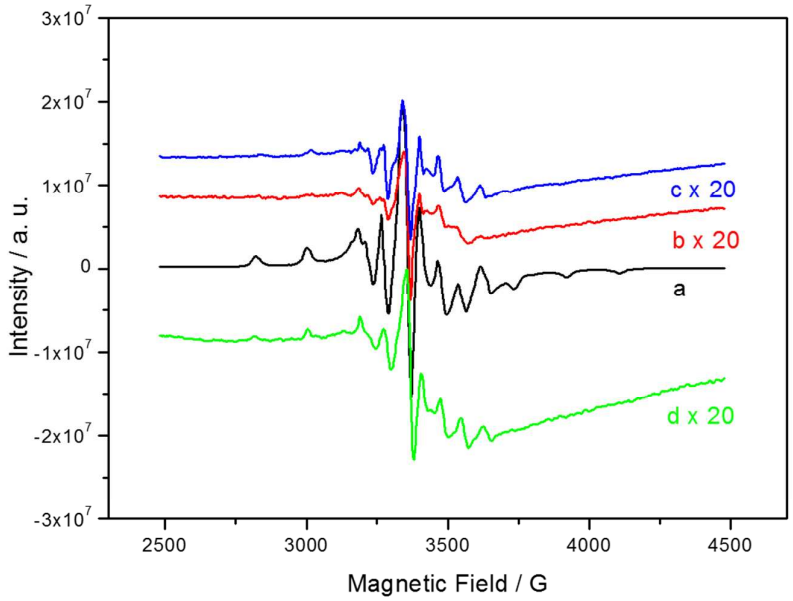

Figure 5. EPR spectra obtained at 100 K in frozen dichloromethane matrix of: complex **1** [VO(acac)(H-BIAN)]Cl (black line, a); **1** + tbhp (red line, b); **1** + cy8 + tbhp (blue line, c); **1** + cy8 + tbhp, 24 hours later (green line, d). As the intensities are different, the less intense spectra (b, c and d) were multiplied by a factor of 20. The integration areas, obtained from the corresponding second derivative spectra, are (a.u.): 2.87 x 10^9 (a), 2.28 x 10^8(b), 2.33 x 10^8 (c), and 4.76 x 10^8 (d).

Cyclic voltammetry studies

1 mM solutions of the vanadium(IV) complexes [VO(acac)(H−BIAN)]Cl (**1**) and the precursor [$VO(acac)_2$] were prepared in supporting electrolyte (0.1 M TBA[PF_6] in acetonitrile and voltammograms of the Pt electrode were obtained at the sweep rate of 50 mV/s in the potential range of -1.5 to 1.5 V. Both complexes display an irreversible oxidation process at high potentials which is not present in the H−BIAN ligand, and can be assigned to the oxidation of V(IV) to V(V). The oxidation potential E_{ox} increases from 0.91 V in the neutral [$VO(acac)_2$] to 1.04 V in the cationic [VO(acac)(H−BIAN)]$^+$ (**1**$^+$) as expected, confirming that it is more difficult to oxidize this latter species.

View Article Online
DOI: 10.1039/C4DT03174A

DFT calculations

The mechanism of the epoxidation reaction was investigated by means of DFT calculations [21] (GAUSSIAN 03[22], see Computational Details). As mentioned in the Introduction, literature data are not very clear about the nature of the catalyst when the precursor is a vanadyl complex. It has been shown that V(V) species can be recovered after the catalysis but they are inactive,[11a,12] and we demonstrated that the VO(IV) species remain in solution after adding tbhp (EPR). Mass spectrometry studies led to its identification as $[VO(acac)(H-BIAN)]^+$ ($\mathbf{1}^+$).

The first step in our mechanism proposal corresponds to addition of the oxidant (methylhydroperoxide in the calculations) to the catalyst precursor, complex $\mathbf{1}^+$. This is an endergonic reaction with a calculated ΔG of 30 kJ.mol^{-1} (Eq. 1).

$[VO(acac)(H-BIAN)]^+$ ($\mathbf{1}^+$) + MeOOH → $[VO(acac)(H-BIAN)(MeO\mathit{O}H)]^+$ (**A**) ΔG = 30 kJ.mol^{-1} (Eq. 1)

In the resulting species, **A**, the methylhydroperoxide coordinates the metal by means of its terminal O-atom, occupying the sixth coordination position, *trans* to the vanadyl oxygen in a distorted octahedral geometry.

From **A**, the formation of the catalytic active species follows a three step mechanism, in which the acac ligand is protonated and lost as acetylacetone (Hacac). The corresponding free energy profile is represented in Figure 6.

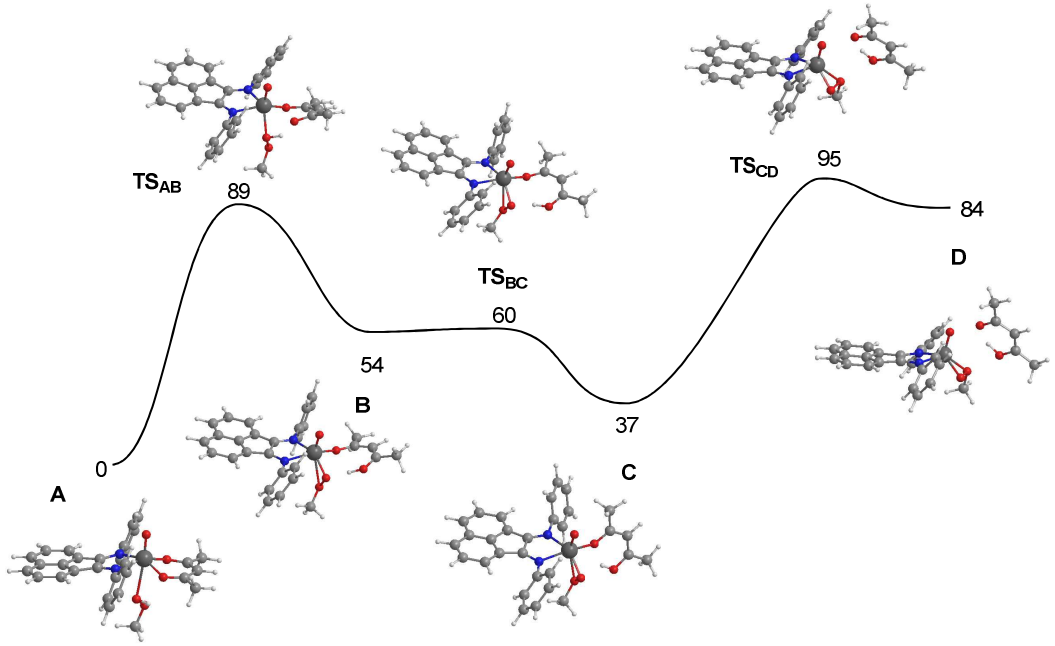

Figure 6. Free energy profile (kJ.mol^{-1}) for the formation of the catalytic active species, $[VO(H-BIAN)(\kappa^2\text{-}\mathit{O,O}\text{-MeOO})]^+$ (**D**), from $[VO(acac)(H-BIAN)(MeO\mathit{O}H)]^+$ (**A**).

View Article Online
DOI: 10.1039/C4DT03174A

In the first step of the mechanism, from **A** to **B**, the methylperoxide transfers a proton to the acac ligand. $MeOO^-$ becomes a formally negative κ^2-OO ligand, while acac becomes acetylacetone (Hacac). The second step involves a rearrangement of the hydrogen bonds in the two ligands, $MeOO^-$ and Hacac. The O•••H-O hydrogen bonds between the OH group in acac and the methylperoxide becomes an internal O•••H-O bond in acetylacetone. Finally, in the third step there is loss of acetylacetone, leaving Hacac and $[VO(H-BIAN)(\kappa^2\text{-}O,O\text{-}MeOO)]^+$ in **D**. Actually, this last complex is similar to the catalyst precursor ($\mathbf{1}^+$) but with a methylperoxide ligand κ^2-OO coordinated, substituting the acac ligand of the initial complex.

The path illustrated in Figure 6 presents a free energy barrier of 95 $kJ.mol^{-1}$ being, thus, accessible in the experimental conditions used for the reaction (see above).

From **D** to **E**, the Hacac is replaced by one ethylene molecule (the olefin substrate used in the calculations). This is a practically energy neutral process (ΔG = 2 $kJ.mol^{-1}$) as, perhaps, might be expected since the complex remains as $[VO(H-BIAN)(\kappa^2\text{-}O,O\text{-}MeOO)]^+$, and Hacac and ethylene are not coordinated. Epoxidation occurs in one single step (Figure 7) from **E** with ethylene attacking the *distal* O-atom of the methylperoxide, following the Sharpless type mechanism.[23] This is a clearly exergonic reaction (ΔG = –231 $kJ.mol^{-1}$) with a free energy barrier of only 72 $kJ.mol^{-1}$, and is quite feasible in the experimental conditions. In the product, **F**, both the recently formed epoxide and methoxide bind to the metal through their O-atom.

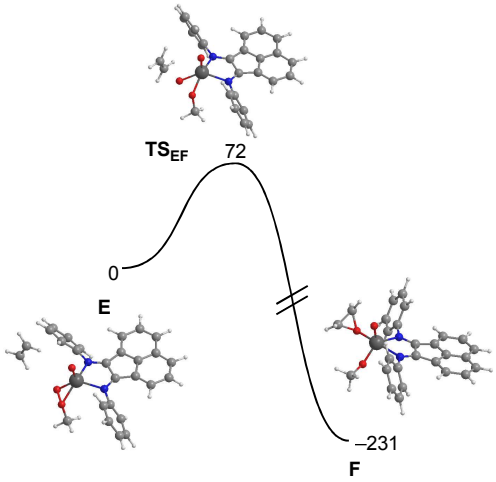

Figure 7. Free energy profile ($kJ.mol^{-1}$) for the epoxidation reaction based external attack of olefin on intermediate **E**, $[VO(H-BIAN)(\kappa^2\text{-}O,O\text{-}MeOO)]^+$ plus ethylene.

Although the epoxidation reaction is finished in **F**, as the product is already formed, a series of ligand exchange reaction will still have to happen in order to close the catalytic cycle. The first one

View Article Online
DOI: 10.1039/C4DT03174A

is the exchange between epoxide and the methylhydroperoxide, releasing the reaction product (epoxide) and acquiring a new oxidant molecule to be used in the following reaction. This reaction is represented in Eq. 2 and has a free energy balance of 18 kJ.mol^{-1}.

$[VO(H-BIAN)(MeO)(OCH_2CH_2)]^+$ (**F**) + MeOOH → $[VO(H-BIAN)(MeO)(MeOOH)]^+$ (**G**) + OCH_2CH_2 ΔG = 18 kJ.mol^{-1} (Eq. 2)

The methylhydroperoxide ligand coordinates the vanadium in **G** by its *distal* oxygen, while the four remaining coordination positions are occupied by the methoxide, the oxide and the two N-atoms of BIAN, all already present in **F**. The geometry of **G** is better described as a distorted trigonal bipyramid with the axial positions defined by the methylhydroperoxide and one *trans* N-atom of BIAN (N–V–O = 171°).

The reaction proceeds by proton transfer from the methylhydroperoxide to the methoxide ligand, through a very facile process with a free energy barrier of only 17 kJ.mol^{-1} and a ΔG of –21 kJ.mol^{-1} (Figure 8) which converts **G** in **H**.

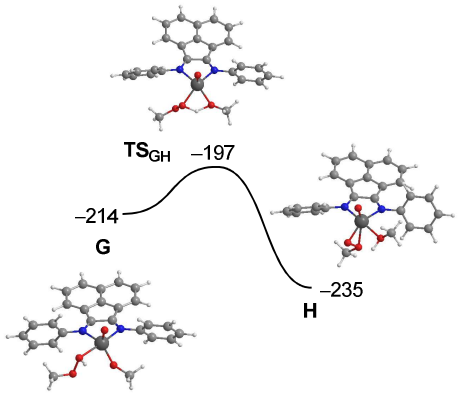

Figure 8. Free energy profile (kJ.mol^{-1}) for the intramolecular proton exchange between $[VO(H-BIAN)(MeO)(MeOOH)]^+$ (**G**) and $[VO(H-BIAN)(MeOH)(MeOO)]^+$ (**H**). The energy values are referred to **E**.

Exchange of methanol, the by-product from the decomposition of the methylhydroperoxide, with a fresh molecule of substrate completes the catalytic cycle (Scheme 4).

View Article Online
DOI: 10.1039/C4DT03174A

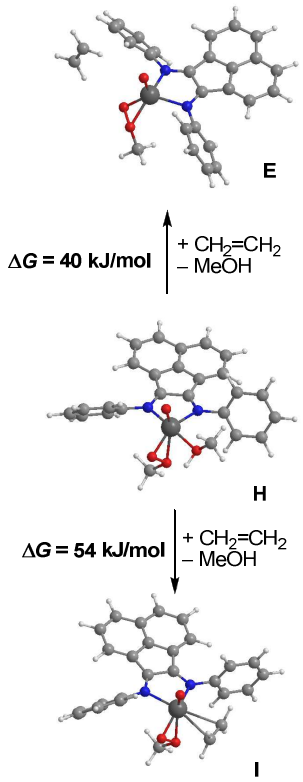

Scheme 4

This may occur by regenerating **E**, where ethylene is not coordinated to [VO(H−BIAN)(κ^2-*O,O*-MeOO)]$^+$ (top of Scheme 4), and immediately closing the cycle, to repeat the mechanism previously described. The corresponding transformation (**H** to **E**) is endergonic with a Δ*G* of 40 kJ.mol^{-1}. As mentioned above, this mechanism based on **E** as active species follows the Sharpless pathway and is an *outer sphere* path[23] since it does not involves direct coordination of the substrate to the metal. Alternatively, one may consider the possibility of coordinating the incoming ethylene molecule to the metal (**I**, bottom of Scheme 4). The methylhydroperoxide ligand remains κ^2-OO coordinated and the ethylene molecule occupies the adjacent coordination position (**I**). This reaction is only 14 kJ.mol^{-1} less favorable than the previous one (forming **E**) and a mechanism involving **I** as active species is also possible. This will be an *inner sphere* process (Mimoun type mechanism),[24] since the olefin coordinates to vanadium, and the multi-step profile calculated is represented in Figure 9.

View Article Online
DOI: 10.1039/C4DT03174A

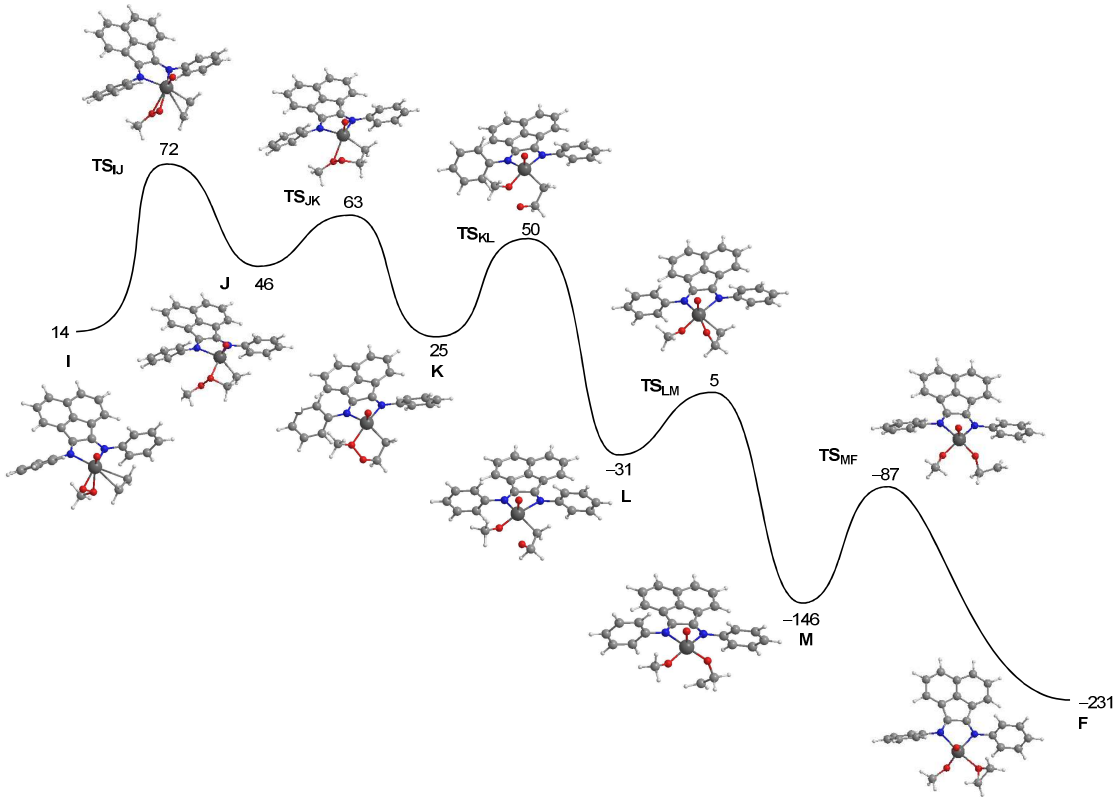

Figure 9. Free energy profile (kJ.mol^{-1}) for the epoxidation reaction based on the ethylene complex **I**. The energy values are referred to **E.**

The first step of the mechanism is a cycloaddition of the C=C bond of the olefin to the V–O bond, from **I** to **J**, and resulting in a four-member metallacyle, V–O–C–C. This metallacycle is expanded from four- to five-members (V–O–O–C–C) in the second step of the mechanism, from **J** to **K**, by means of a coordination shift of vanadium from the distal to the proximal O-atom of the methylperoxide.

In the third step (**K** to **L**), there is a homolytic cleavage of the O–O bond forming an intermediate (**L**) with two new ligands, one methoxide (MeO) and one alkyl with a dangling O-atom ($CH_2CH_2O^{\bullet}$), resulting from the two fragments of the metallacycle. In the following step, from **L** to **M**, the coordination of the latter ligand shifts from C- to O- and it becomes an alkoxide with a dangling carbon end, in **M**: $OCH_2CH_2^{\bullet}$. In the final step, the C–O bond in the coordinated epoxide of complex **F** is formed. The overall process is clearly exergonic (ΔG = –245 kJ.mol^{-1}) and the highest barrier is the one associated with the first step (**TS$_{IJ}$**, 58 kJ.mol^{-1}). Curiously, the energy of the corresponding transition state, **TS$_{IJ}$**, differs only 0.4 kJ/mol from the energy of the transition state calculated for the epoxidation reaction *via* the *outer sphere* mechanism (**TS$_{EF}$**, in Figure 7), indicating that the two mechanisms are competitive and most probably occur simultaneously.

View Article Online
DOI: 10.1039/C4DT03174A

Interestingly, the intermediates **L** and **M**, in the path represented in Figure 9 are formally V(V) complexes with the unpaired electron located mostly in the dangling atom of the CH_2CH_2O ligand, the oxygen atom in the case of intermediate **L**, and the carbon atom in the case of **M**. This is clearly reflected in the spin density represented in Figure 10 for these two intermediates.

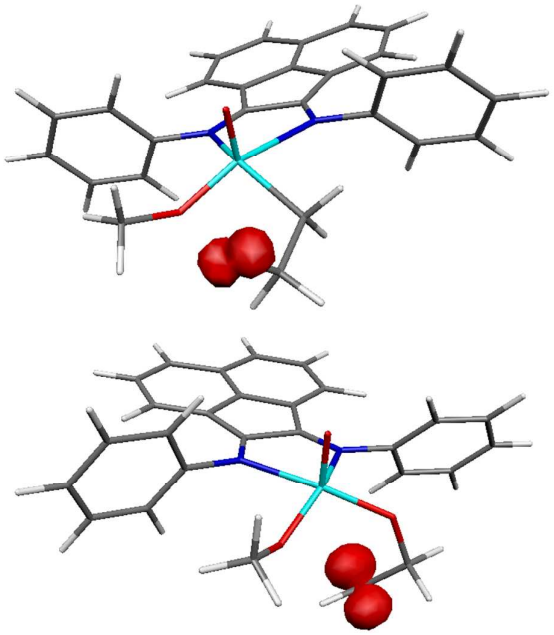

Figure 10. Spin density of intermediates **L** (top) and **M** (bottom).

Inhibition of the catalyst activity by alcohol can be explained by the exchange reaction depicted in Scheme 4, representing the closing of the cycles through the replacement of methanol by one new molecule of substrate. In fact, those are endergonic processes and the corresponding equilibria will be shifted backwards by increasing concentrations of alcohol, since this is a reaction product.
The formation of the active species from the precursor complex, as well as the catalytic cycle are shown in Scheme 5, emphasizing the relevant intermediates. It also stresses the role of the active complex $[VO(H-BIAN)(\kappa^2\text{-}O,O\text{-}MeOO)]^+$, which appears **D** at the end of the reaction MeOOH that also releases Hacac. This molecule remains hydrogen bonded to the cation and is displaced by the substrate, first weakly bound in **E** and giving the reaction product (**F**). The amounts of **D** and **E** will depend on the concentration of the substrate.

View Article Online
DOI: 10.1039/C4DT03174A

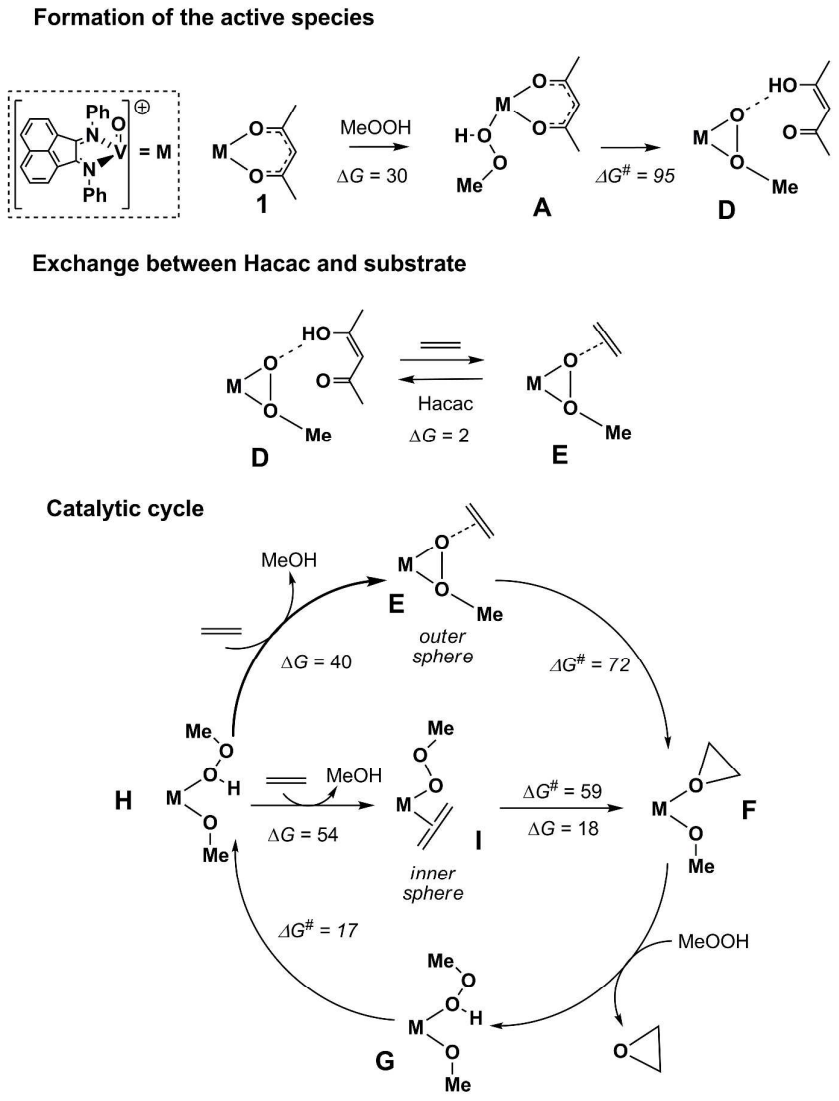

Scheme 5

Conclusions

The new oxovanadium(IV) complexes [VO(acac)(R−BIAN)]Cl (BIAN = 1,2−bis{(R−phenyl)imino}acenaphthene, R = H, **1**; CH_3, **2**; Cl, **3**) were found to be active catalyst precursors for the epoxidation of cyclohexene, *cis*-cyclooctene, and styrene using either tbhp or H_2O_2 as oxidants, and for the epoxidation of enantiopure olefins with tbhp. All led to high selectivity toward epoxide formation, and diols were never observed. In olefins such as limonene with two C=C bonds, the secondary olefin was preferred to the terminal one.

Kinetic studies indicated a first order dependency on the oxidant (tbhp or H_2O_2) in all metal complexes, with positive $\Delta H^{\neq}$ and very negative $\Delta S^{\neq}$ suggesting an associative mechanism. Mass

View Article Online
DOI: 10.1039/C4DT03174A

spectrometry studies of the reaction of complex **1** and tbhp allowed the isolation and detection of a V(IV) complex $[VO(acac)(H-BIAN)]^+$. EPR experiments demonstrated that V(IV) persists in solution after addition of tbhp or tbhp and Cy8, for at least 48 hours (weaker signal), even though most of the initial complex has been oxidized suggesting that a V(IV) species may be involved in catalysis. Cyclic voltammetry experiments showed that it is more difficult to oxidize the cationic complex $\mathbf{1}^+$ than $[VO(acac)_2]$, supporting the previous statement. Based on this evidence, the possibility of a V(IV) catalyzed reaction mechanism was investigated by means of DFT calculations. After the formation of the V(IV) active species in an associative step, the results indicate two competitive processes that probably occur simultaneously: an *outer sphere* path with external attack of the olefin at the coordinated peroxide, and an *inner sphere* mechanism based on a complex with coordinated substrate. The largest barrier (95 $kJ.mol^{-1}$) occurs in the formation of the catalytic active species, $[VO(H-BIAN)(\kappa^2\text{-}O,O\text{-}MeOO)]^+$ (**D**).

Experimental

All preparations and manipulations were performed using standard Schlenk techniques under nitrogen. Commercial grade solvents were dried and deoxygenated by standard procedures (hexane and diethyl ether over Na/benzophenone ketyl; CH_3CN over CaH_2), distilled under nitrogen, and kept over 4 Å molecular sieves (3 Å for CH_3CN). Tbhp, hydrogen peroxide, ciclooctene, ciclohexene, styrene, *S*(−)−pinene, *R*(+)−pinene, *S*(−)−limonene and *R*(+)−limonene, acenaphthenequinone, aniline, p−toluidine, and 4−chloroaniline were purchased from Aldrich and used as received. $[VO(acac)_2]$ was prepared by a method described in the literature.[25] The synthesis of the vanadyl complexes was adapted from the literature.[26]

^1H and ^{13}C solution NMR spectra were obtained at 400.13 MHz and 100.62 MHz, respectively, with a Bruker Avance 400 spectrometer using $CDCl_3$ and CD_3OD as solvents. Chemical shifts are quoted in ppm from TMS.

FTIR spectra were measured with a Nicolet Nexus 6700 FTIR spectrometer as KBr pellets in transmission mode, with 2 cm^{-1} resolution. Microanalyses were performed at CACTI at the University of Vigo. UV-VIS spectra were measured in a Shimadzu spectrometer in solution of MeCN or CH_2Cl_2.

Mass Spectrometry experiments

All ESI–MS experiments were performed using an ApexQe FTICR Mass Spectrometer from Bruker Daltonics (Billerica, MA, USA) equipped with an electrospray ion source and a 7 T actively shielded superconducting magnet. The samples were introduced, by means of an infusion pump from KD Scientific (Holliston, MA, USA), with a flow rate of 120 $\mu L \cdot h^{-1}$. The vacuum was

View Article Online
DOI: 10.1039/C4DT03174A

maintained by means of mechanical vacuum pumps followed by turbomolecular pumps in two different regions: ion source (maintained ~6.0×10^{-6} mbar) and cell region (maintained ~4.0×10^{-10} mbar).The mass spectrometer was calibrated using a 2.8×10^{-6} mol·L^{-1} solution of polyethylenglycol acquired from Sigma-Aldrich (St. Louis, MO, USA) in HPLC grade methanol acquired from Panreac (Barcelona, Spain) and acidified with 0.1% (v/v) of formic acid acquired from Fluka (Seelze, Germany).

The mass spectra were acquired in the positive ion broadband mode, with an acquisition size of 512k, in the mass range of 50–500. The nebulizer gas flow rate was set to 2.5 L·min^{-1}, the dry gas flow rate was set to 4.0 L·min^{-1} at a temperature of 493 K. The capillary voltage was set to 4200 V and the spray shield voltage was set to 3800 V. The ion source optics, collision cell and ICR cell parameters were optimized to ensure the highest abundance possible for the ions of interest. All mass spectra presented are the average of 32 mass spectra. The ions were accumulated in the collision cell during 1.0 s prior to their transfer to the ICR cell. The MS^2 experiments were performed using Argon, acquired from Praxair (Danbury, CT, USA), as collision gas at a flow rate of 0.30 L·s^{-1}. The collision cell voltage was varied for each compound in order to find the appropriate value.

The MS kinetic experiments were carried out by isolating the ion of interest in the ICR cell and by introducing the reactants (tbhp or *cis*-cyclooctene) through a leak valve. The valve was opened until the pressure in the cell achieved a stationary pressure of 10^{-8} mbar. Prior to the time delay of interest the ions were thermalized to achieve consistent results.

Synthesis

Preparation of the ligands (L1-L3)

To a suspension of acenaphthenequinone ($C_{12}H_6O_2$) (3.28 mmol, 0.6 g) in acetonitrile (MeCN) (30 mL) was added 5.3 mL of acetic acid. This mixture was stirred under reflux until all the acenaphthenequinone was dissolved. A solution of 4-chloroaniline, aniline or p-toluidine (7.1 mmol) in acetonitrile was then added, and the new solution was stirred for 4 h 30 min under reflux. The ligand precipitated after cooling the solution in the fridge, and was recrystallized from acetonitrile.

1,2−bis[(phenyl)imino]acenaphthene (p−BIAN, **L1**)

Yield: 0.932 g, 86%. $C_{24}H_{16}N_2$ (332.40) calcd: C 86.72, H 4.85, N 8.43, found: C 86.49, H 4.43, N 8.00. IR (ν cm^{-1}): 3082 (vw), 3054 (w), 3018 (vw), 1737 (vs), 1653 (vs), 1593 (vs), 1484 (s), 1423 (m), 1360 (vw), 1278 (m), 1230 (m), 1176 (w), 1072 (m), 1026 (m), 914 (m), 893 (m), 830 (s), 803 (w), 777 (vs), 765 (vs), 696 (vs).

View Article Online
DOI: 10.1039/C4DT03174A

^{1}H NMR (400.13 MHz, $CDCl_3$, r.t., δ ppm): 7.01 (d, 4H, Ph (4)), 7.21 (d, 2H, Ph (6)), 7.34-7.42 (m, 4H, Ph (5)), 7.74 (t, 2H, BIAN (2)), 7.92 (d, 2H, BIAN (3)), 8.08–8.11 (dd, 2H, BIAN (1)). UV-Vis (MeCN solution): λ_{max} = 304 nm ($\varepsilon = 1.833\times10^5$ $dm^2\cdot mol^{-1}$).

1,2−bis[(4−methylphenyl)imino]acenaphthene (mp−BIAN, **L2**)

Yield: 0.908 g, 77%. $C_{26}H_{20}N_2$ (360.45) calcd: C 86.64, H 5.59, N 7.77, found: C 86.30, H 7.33, N 5.13. IR (ν cm^{-1}): 3052 (vw), 3022(vw), 2919 (w), 2863 (vw), 1731 (vs), 1657 (s), 1603 (m), 1589 (s), 1501 (vs), 1489 (s), 1419 (m), 1270 (s), 1237 (s), 1177 (m), 1107 (m), 1072 (m), 1031 (m), 1015 (m), 927 (w), 911 (m), 821 (vs), 779 (s).

^{1}H NMR (400.13 MHz, $CDCl_3$, r.t., δ ppm): 2.37 (s, 6H, CH_3), 6.95 (t, 4H, Ph (4)), 7.20 (d, 4H, Ph (5)), 7.74 (t, 2H, BIAN (2)), 7.80-7.94 (dd, 2H, BIAN (3)), 8.09 (dd, 2H, BIAN (1)). UV-Vis (MeCN solution): λ_{max} = 303 nm ($\varepsilon = 1.001\times10^5$ $dm^2\cdot mol^{-1}$).

1,2−bis[(4−chlorophenyl)imino]acenaphthene (cp−BIAN, **L3**)

Yield: 1.150 g, 87%. $C_{24}H_{14}N_2Cl$ (401.28) calcd: C 71.83, H 3.52, N 6.98, found: C 71.63, H 3.16, N 6.55. IR (ν cm^{-1}): 3056 (vw), 1731 (vs), 1658 (s), 1588 (m), 1479 (vs), 1420 (w), 1275 (m), 1228 (m), 1172 (w), 1090 (m), 1071 (w), 1032 (m), 1012 (m), 910 (w), 827 (vs), 776 (s), 721 (w), 648 (w), 589 (w), 529 (m).

^{1}H NMR (400.13 MHz, $CDCl_3$, r.t., δ ppm): 6.99 (t, 4H, Ph (4)), 7.39 (d, 4H, Ph (5)), 7.77 (t, 2H, BIAN 2), 7.97 (d, 2H, BIAN 1), 8.13 (dd, 2H, BIAN (3)). UV-Vis (solution MeCN): λ_{max} = 304 nm ($\varepsilon = 4.825\times10^4$ $dm^2\cdot mol^{-1}$).

Preparation of the complexes (1−3)

A solution of $[VO(acac)_2]$ (1 mmol, 265 mg), in methanol (10 mL) was treated with a solution of each of the ligands **L1**-**L3** (1 mmol) in methanol and 1 mmol of HCl, and stirred for 4 h under reflux. The complex was obtained by evaporation of the solvent. It was washed several times with hexane and diethyl ether, dried under vacuum, and recrystallized from methanol/diethyl ether.

[VO(acac)(R−BIAN)]Cl (R = H, **1**)

Yield: 0.469 g, 88%. $C_{29}H_{23}N_2O_3VCl$ (533.44) calcd: C 65.24, H 4.32, N 5.25, found: C 64.89, H 4.65, N 4.91. IR (ν cm^{-1}): 3056 (w), 2933 (w), 2831 (w), 1566 (vs), 1524 (s), 1486 (s), 1363 (vs), 1284 (s), 1187 (m), 1066 (m), 1027 (m), 1000 (s), 932 (m), 834 (m), 778 (s), 694 (m), 586 (m), 464 (w).

View Article Online
DOI: 10.1039/C4DT03174A

^{1}H NMR (400.13 MHz, $CDCl_3$, r.t., δ ppm): 1.93-2.52 (d bd, 6H, acac–CH_3), 6.42 (s bd, 1H, acac–H), 6.83-8.27 (m, 16H, BIAN).
UV-Vis (solution MeCN): λ_{max} = 306 nm ($\varepsilon = 2.246\times10^5$ $dm^2\cdot mol^{-1}$).

[VO(acac)(R−BIAN)]Cl (R = Me, **2**)
Yield: 0.480 g, 86%. $C_{31}H_{27}N_2O_3VCl$ (561.44) calcd: C 66.26, H 4.84, N 4.98, found: C 66.05, H 4.53, N 4.94. IR (ν cm^{-1}): 3042(vw), 2972 (vw), 2925 (vw), 1560 (vs), 1523 (s), 1502 (s), 1286 (vs), 1189 (m), 1019 (m), 995 (s), 937 (m), 834 (m), 784 (s), 488 (m).
^{1}H NMR (400.13 MHz, $CDCl_3$, r.t., δ ppm): 2.00 (t bd, 6H, acac–CH_3), 2.33 (d, 6H, BIAN–CH_3), 6.47 (s bd, 1H, acac–H), 6.93–6.99 (dd bd, 2H, BIAN-4), 7.17–7.25 (m, 4H, BIAN-5, BIAN-2), 7.20 (s, 1H, Ph 12), 7.54–7.78 (m, 4H, BIAN-1, BIAN-3). UV-Vis (solution MeCN): λ_{max} = 306 nm ($\varepsilon = 1.582\times10^5$ $dm^2\cdot mol^{-1}$).

[VO(acac)(R−BIAN)]Cl (R = Cl, **3**)
Yield: 0.543 g, 90%. $C_{29}H_{21}N_2O_3VCl_3$ (602.44) calcd: C 57.78, H 3.51, N 4.65, found: C 57.32, H 3.51, N 4.48. IR (ν cm^{-1}): 3057 (vw), 2931 (w), 2832 (w), 1566 (vs), 1524 (s), 1485 (s), 1363 (vs), 1283 (s), 1191 (s), 1090 (s), 1014 (s), 979 (s), 938 (m), 833 (m), 789 (vs), 746 (m), 680 (m), 589 (m), 462 (m).
^{1}H NMR (400.13 MHz, $CDCl_3$, r.t., δ ppm): 1.94-2.46 (d bd, 6H, acac–CH_3), 6.48 (s bd, 1H, acac–H), 7.03–8.24 (m, 14H, BIAN).
UV-Vis (solution MeCN): λ_{max} = 307 nm ($\varepsilon = 2.314\times10^5$ $dm^2\cdot mol^{-1}$).

Catalytic epoxidation of *cis*-cyclooctene, cyclohexene, and styrene in the presence of 1−3 with tbhp or H_2O_2

Cyclooctene (7.3 mmol), cyclohexene (9.7 mmol), or styrene (7.7 mmol) and *t*−butyl hydroperoxide (200 mol %, 5.5 M solution in decane) or H_2O_2 (200 mol %, 30% solution) were mixed in the presence of complexes **1−3** (1 mol %) in a glass reactor, at 328 K, and vigorously stirred. Conversion was monitored by taking samples and analyzing them by gas chromatography using a capillary column (HP−5) and a flame ionization detector. Cyclohexene, *cis*-cyclooctene, and styrene epoxides were quantified using NMR spectroscopy.

View Article Online
DOI: 10.1039/C4DT03174A

Catalytic epoxidation of *R*(+), *S*(+)−limonene, *R*(−), *S*(−)−pinene in the presence of 1−3 with tbhp.

S(−)−, *R*(+)−pinene, *S*(−)−, and *R*(+)−limonene (5.87 mmol), and *t*−butyl hydroperoxide (200 mol %, 5.5 M solution in decane) were mixed in the presence of complexes **1−3** (1 mol %) in a glass reactor, at 328 K, and vigorously stirred. Conversion was monitored by taking samples and analyzing them by gas chromatography using a capillary column (HP−1) and a flame ionization detector. The respective epoxides were quantified using NMR spectroscopy.

UV-vis Kinetic studies

All kinetic measurements were carried out using a large excess of tbhp (pseudo−first−order conditions). Typically, an appropriate small quantity of concentrated tbhp in decane (5.5 M) was added to a thermostated UV quartz cell, at 298, 303, 313, 323, 328 K, containing an appropriate amount of a solution of the metal complex in CH_3CN in order to obtain a total volume of 3 mL with a final concentration of [VO(acac)(R−BIAN]Cl (**1**) equal to $1x10^{-4}$ M. The product formation was monitored against time at regular time intervals by following absorbance changes at 302 nm on a UV−VIS Shimadzu spectrometer with a variable temperature cell and stirring.

Electron paramagnetic resonance spectroscopy (EPR). Samples of the various experiments were prepared by dissolution of the reagents in dichloromethane and placed in capillary tubes, which were then introduced in the quartz EPR tubes. The samples to be recorded at room temperature were prepared, placed in the spectrometer and analyzed. The samples to be recorded in frozen solution were prepared, frozen in liquid nitrogen, and placed in the spectrometer at the desired temperature. EPR spectra were recorded using a Bruker ELEXSYS E500 spectrometer operating at 9 GHz (X-band) equipped with a variable temperature unit (ER 4B1 VT), available at Laboratório de Ressonância Magnética Electrónica (Centro de Estudos de Materiais da Universidade do Porto). EPR spectra were obtained in the following experimental conditions: microwave frequency of (9.4505 GHz), modulation frequency of 100 kHz, microwave power of 6 mW, modulation amplitude of 4 G and 60 dB of receiver gain. Room temperature spectra were recorded with acquisition time of 5 s, 5 scans at (296 ± 1) K and spectra acquired at (100 ± 1) K were recorded with acquisition time of 100 s, 5 scans. The spectra were simulated with the computer suite program Bruker WinEPR/SimFonia.

Cyclic voltammetry studies. All electrochemical measurements were performed using a *CHI* Electrochemical Analyser-620A Model controlled by a computer at room temperature in an one-compartment electrochemical Teflon cell. A polycrystalline platinum (Pt) working electrode (area A

View Article Online
DOI: 10.1039/C4DT03174A

= 0.008 cm^2), a platinum foil counter electrode (area 2.0 cm^2) and a saturated calomel electrode (SCE) as reference electrode were used. Before each experiment, a mirror-finishing platinum surface was generated by hand-polishing the electrode in an aqueous suspension of successively finer grades of alumina (down to 0.05 μm). All the solutions were deoxygenated directly in the electrochemical cell with nitrogen gas (N_2).

The electrochemical studies were performed at 0.050V/s sweep rate, in the potential range of -1.5 – 1.5 V. To minimize solution resistance and promote the flow of electrons, the electrolyte solution used was 0.1 M tetrabutylammonium hexafluorophosphate (TBA[PF_6]) in acetonitrile (ACN). 1 mM solutions of the vanadium (IV) complex (**1**) and precursor [$VO(acac)_2$] were prepared in $TBAPF_6$/ ACN electrolyte.

Computational Details. All DFT[21] calculations were performed using the GAUSSIAN 03 software package,[22] and the PBE1PBE functional, without symmetry constraints. That functional uses a hybrid generalized gradient approximation (GGA), including 25% mixture of Hartree−Fock[27] exchange with DFT exchange-correlation, given by Perdew, Burke and Ernzerhof functional (PBE).[28] The optimized geometries were obtained with the LanL2DZ basis set[29] augmented with an f-polarization function,[30] for V, and a standard 6−31G(d,p)[31] for the remaining elements (basis b1). Transition state optimizations were performed with the Synchronous Transit-Guided Quasi-Newton Method (STQN) developed by Schlegel *et al*,[32] following extensive searches of the Potential Energy Surface. Frequency calculations were performed to confirm the nature of the stationary points, yielding one imaginary frequency for the transition states and none for the minima. Each transition state was further confirmed by following its vibrational mode downhill on both sides and obtaining the minima presented on the energy profile. The electronic energies (E_{b1}) obtained at the PBE1PBE/b1 level of theory were converted to free energy at 298.15 K and 1 atm (G_{b1}) by using zero point energy and thermal energy corrections based on structural and vibration frequency data calculated at the same level.

Single point energy calculations were performed using a standard 6-311++G(d,p)[33] basis set for all the elements, and the geometries optimized at the PBE1PBE/b1 level. Solvent effects (CH_2Cl_2) were considered in the PBE1PBE/6-311++G(d,p)//PBE1PBE/b1 energy calculations using the Polarizable Continuum Model (PCM) initially devised by Tomasi and coworkers[34] as implemented on GAUSSIAN 03.[35] The molecular cavity was based on the united atom topological model applied on UAHF radii, optimized for the HF/6-31G(d) level.

The free energy values presented along the text (G_{b2}^{soln}) were derived from the electronic energy values obtained at the PBE1PBE/b2//PBE1PBE/b1 level, including solvent effects (E_{b2}^{soln}), according to the following expression:

View Article Online
DOI: 10.1039/C4DT03174A

$$G_{b2}^{soln} = E_{b2}^{soln} + G_{b1} - E_{b1}$$

Acknowledgements

We thank FCT, POCI, and FEDER for funding (projects POCI/QUI/58925/2004, PEst-OE/QUI/UI0100/2014, and PEst-OE/QUI/UI0612/2014). The authors also thank the Portuguese National Mass Spectrometry Network (REDE/1501/REM/2005). The Bruker ELEXYS EPR spectrometer was purchased under the framework of QREN, through project NORTE-07-0162-FEDER-000048. To all financing sources the authors are greatly indebted.

References

[1] J. J. R. Fraústo da Silva, R. J. P. Williams, *The Biological Chemistry of the Elements*, Clarendon Press, Oxford, **1991**.
[2] a) H. Elias, S. Schwartze-Eidan, *Inorg. Chem.* **2003**, *42*, 2878-2885. b) Y. Tayika, K. Tsuge, Y. Sasaki, *Dalton Trans.* **2005**, 1438-1447. c) A. D. Keramidas, A. B. Papaioannou, A. Vlahos, T. A. Kabanos, G. Bonas, A. Makriyannis, C. P. Rapropoulou, A. Terzis, *Inorg. Chem.***1996**, *35*, 357-367.
[3] Thompson, K. H., Orvig, C., *J. Inorg. Biochem.* **2006**, *100*, 1925-1935
[4] a) A. G. J. Ligtenbarg, R. Hage, B. L. Feringa, *Coord. Chem. Rev.* **2003**, *237*, 89-101. b) C. Bolm, *Coord. Chem. Rev.* **2003**, *237*, 245-256.
[5] M. R. Maurya, *Coord. Chem. Rev.* **2003**, *237*, 163-181.
[6] a) E. S. Gould, R. R. Hiatt, K. C. Irwin, *J. Am. Chem. Soc.* **1968**, *90*, 4573-4579. b) J. Hartung, M. Greb, *J. Organomet. Chem.* **2002**, *661*, 67-84. c) G. B. Shul´pin, Y. N. Kozlov, G. V. Nizova, G. Süss-Fink, S. Stanislas, A. Kitaygorodskiy, V. S. Kulikova, *J. Chem. Soc., Perkin Trans. 2* **2001**, 1351-1371.
d) K. P. Bryliakov, E. P. Talsi, S. N. Stas´ko, O. A. Kholdeeva, S. A. Popov, A.V. Tkachev, *J. Mol. Catal., A: Chem.* **2003**, *194*, 79-88.e) M. Sutradhar, M. V. Kirillova, M. F. C. Guedes da Silva, L. M. D. R. S. Martins, A. J. L. Pombeiro, *Inorg. Chem.* **2012**, *51*, 11229-11231. f) A. M. Fayed, S. A. Elsayed, A. M. El-Hendawy, M. R. Mostafa, *Spectrochim. Acta Part A: Mol. Biomol. Spectr*. **2014**, *129*, 293–302. g) P. Adão, M. L. Kuznetsov, S. Barroso, A. M. Martins, F. Avecilla, J. Costa Pessoa *Inorg. Chem.* **2012**, *51*, 11430-11449.
[7] S. Mohebbi, F. Nikpour, S. Raiati, *J. Mol. Catal., A: Chem.* **2006**, *256*, 265-268.
[8] T. Joseph, D. Srinivas, C. S. Gopinath, S. B. Halligudi, *Cat. Lett*. **2002**, *83*, 209-214.
[9] O. Bortolini, V. Conte, *Mass Spect. Rev.* **2006**, *25*, 724-740.
[10] a) F. E. Kühn, M. Groarke, É. Bencze, E. Herdtweck, A. Prazeres, A. M. Santos, M. J. Calhorda, C. C. Romão, I. S. Gonçalves, A. D. Lopes, M. Pillinger, *Chem. Eur. J.* **2002,** *8*, 2370-2383. b) L. F. Veiros, Â. Prazeres, P. J. Costa, C. C. Romão, F. E. Kühn, M. J. Calhorda, *Dalton Trans.* **2006**, 1383-1389. c) J. C. Alonso, P. Neves, M. J. Pires da Silva, S. Quintal, P. D. Vaz, C. Silva, A. A. Valente, P. Ferreira, M. J. Calhorda, V. Félix, M. G. B. Drew, *Organometallics* **2007**, *26*, 5548–5556.
[11] a) C. K. Sams, K.A. Jørgensen, *Acta Chem. Scand.* **1995**, *49*, 839-847. b) R. Z. Khaliullin, A. T. Bell, M. Head-Gordon, *J. Phys. Chem. B* **2005**, *109*, 17984-17992.
[12] M. Vandichel, K. Leus, P. van der Voort, M. Waroquier, V. van Speybroeck, *J. Catal.* **2012**, *294*, 1-18.

View Article Online
DOI: 10.1039/C4DT03174A

[13] I. L. Fedushkin, V. A. Chudakova, A. A. Skatova, N. M. Khvoinova, Y. A. Kurskii, T. A. Glukhova, G. K. Fukin, S. Dechert, M. Hummert, H. Schumann**,** *Z. Anorg. Allg. Chem.* **2004**, *630*, 501-507.
[14] W. J. Geary**,** *Coord. Chem. Rev.* **1971**, *7*, 81–122.
[15] K. Nakamoto, *Infrared and Raman spectra of inorganic and coordination compounds*, Wiley New York, **1997**.
[16] X. Li, M. S. Lah, V. L. Pecoraro, *Inorg. Chem.* **1988**, *27*, 4657-4664.
[17] J. A. Bonadies, C. J. Carrano, *J. Am. Chem. Soc.* **1986**, *108*, 4088-4095
[18] F. E. Kuhn, W.-M. Xue, A. Al-Ajlouni, A. M. Santos, S. Zhang, C. C. Romão, G. Eickerling, E. Hertweck, *Inorg. Chem.* **2002**, *41*, 4468-4477.
[19] A. A. Valente, J. Moreira, A. D. Lopes, M. Pillinger, C. D. Nunes, C. C. Romão, F. E. Kuhn, I. S. Gonçalves, *New J. Chem.*, **2004**, *28*, 308-313.
[20] O. Pestovsky, R. van Eldik, P. Huston, J. H. Espenson *Dalton Trans.* **1995**, 133-137.
[21] R. G. Parr, W. Yang, *Density Functional Theory of Atoms and Molecules*, Oxford University Press, New York, **1989**.
[22] Gaussian 03, Revision C.02,M. J. Frisch, G. W. Trucks, H. B. Schlegel, G. E. Scuseria, M. A. Robb, J. R. Cheeseman, J. A. Montgomery, Jr., T. Vreven, K. N. Kudin, J. C. Burant, J. M. Millam, S. S. Iyengar, J. Tomasi, V. Barone, B. Mennucci, M. Cossi, G. Scalmani, N. Rega, G. A. Petersson, H. Nakatsuji, M. Hada, M. Ehara, K. Toyota, R. Fukuda, J. Hasegawa, M. Ishida, T. Nakajima, Y. Honda, O. Kitao, H. Nakai, M. Klene, X. Li, J. E. Knox, H. P. Hratchian, J. B. Cross, C. Adamo, J. Jaramillo, R. Gomperts, R. E. Stratmann, O. Yazyev, A. J. Austin, R. Cammi, C. Pomelli, J. W. Ochterski, P. Y. Ayala, K. Morokuma, G. A. Voth, P. Salvador, J. J. Dannenberg, V. G. Zakrzewski, S. Dapprich, A. D. Daniels, M. C. Strain, O. Farkas, D. K. Malick, A. D. Rabuck, K. Raghavachari, J. B. Foresman, J. V. Ortiz, Q. Cui, A. G. Baboul, S. Clifford, J. Cioslowski, B. B. Stefanov, G. Liu, A. Liashenko, P. Piskorz, I. Komaromi, R. L. Martin, D. J. Fox, T. Keith, M. A. Al-Laham, C. Y. Peng, A. Nanayakkara, M. Challacombe, P. M. W. Gill, B. Johnson, W. Chen, M. W. Wong, C. Gonzalez, and J. A. Pople, Gaussian, Inc., Wallingford CT, 2004.
[23] K. B. Sharpless, J. M. Townsend, *J. Am. Chem. Soc*. **1972**, 94, 295-296.
[24] H. Mimoun, I.Seree de Roch, L. Sajus, *Tetrahedron* **1970**, 26, 37-50.
[25] *Inorganic Experiments*, J. Derek Woollins Ed, VCH, Weinheim, **1994**.
[26] T. A. Fernandes, C. D. Nunes, P. D. Vaz, M. J. Calhorda, P. Brandão, J. Rocha, I. S. Gonçalves, A. A. Valente, L. P. Ferreira, M. Godinho, P. Ferreira *Micro. Meso. Mat.* **2008**, 112, 14–25.
[27] W. J. Hehre, L. Radom, P. V. R. Schleyer, J. A. Pople, *Ab Initio Molecular Orbital Theory*, John Wiley & Sons, NY, 1986.
[28] a) J. P. Perdew, K. Burke, M. Ernzerhof, *Phys. Rev. Lett.* **1997**, *78*, 1396. b) J. P. Perdew, *Phys. Rev. B* **1986**, *33*, 8822–8824.
[29] a) T. H. Dunning Jr., P. J. Hay, *Modern Theoretical Chemistry*, Ed. Schaefer, H. F. III (Plenum, New York, **1976**, vol. 3, p. 1. b) P. J. Hay, W. R. Wadt, *J. Chem. Phys.* **1985**, *82*, 270–283. c) W. R. Wadt, P. J. Hay, *J. Chem. Phys.* **1985**, *82*, 284–298. d) P. J. Hay, W. R. Wadt, *J. Chem. Phys.* **1985**, *82*, 299–310.
[30] A. W. Ehlers, M. Böhme, S. Dapprich, A. Gobbi, A. Höllwarth, V. Jonas, K. F. Köhler, R. Stegmann, A. Veldkamp, G. Frenking, *Chem. Phys. Lett.* **1993**, *208*, 111–114.
[31] a) R. Ditchfield, W. J. Hehre, J. A. Pople, *J. Chem. Phys.* **1971**, *54*, 724–728. b) W. J. Hehre, R. Ditchfield, J. A. Pople, *J. Chem. Phys.* **1972**, *56*, 2257–2261. c) P. C. Hariharan, J. A. Pople, *Mol. Phys.* **1974**, *27*, 209–214. d) M. S. Gordon, *Chem. Phys. Lett.* **1980**, *76*, 163–168. e) P. C. Hariharan, J. A. Pople, *Theor. Chim. Acta* **1973**, *28*, 213–222.
[32] a) C. Peng, P. Y. Ayala, H. B. Schlegel, M. J. Frisch, *J. Comput. Chem.* **1996**, *17*, 49; b) C. Peng, H. B. Schlegel, *Isr. J. Chem*. **1993**, *33*, 449-454.

View Article Online
DOI: 10.1039/C4DT03174A

[33] a) A. D. McClean, G. S. Chandler *J. Chem. Phys.* **1980**, *72*, 5639-5648. b) R. Krishnan, J. S. Binkley, R. Seeger, J. A. Pople *J. Chem. Phys.* **1980**, *72*, 650-654. c) A. J. H.Wachters *J. Chem. Phys.* **1970**, *52*, 1033-1036. d) P. J. Hay *J. Chem. Phys.* **1977**, *66*, 4377-4384. e) K. Raghavachari, G. W. Trucks *J. Chem. Phys.* **1989**, *91*, 1062-1065. f) R. C. Binning Jr., L. A. Curtiss *J. Comp. Chem.*, **1990**, *11*, 1206-1216. g) M. P. McGrath, L. Radom *J. Chem. Phys.* **1991**, *94*, 511-516. h) T. Clark, J. Chandrasekhar, G. W. Spitznagel, P. v. R. Schleyer *J. Comp. Chem.* **1983**, *4*, 294-301. i) M. J. Frisch, J. A. Pople, J. S. Binkley *J. Chem. Phys.* **1984**, *80*, 3265-3269.

[34] a) M. T. Cancès, B. Mennucci, J. Tomasi, *J. Chem. Phys.* **1997**, *107*, 3032-3041. b) M. Cossi, V. Barone, B. Mennucci, J. Tomasi, *Chem. Phys. Lett.* **1998**, *286*, 253-260. c) B. Mennucci, J. Tomasi, *J. Chem. Phys.* **1997**, *106*, 5151-5158.

[35] a) J. Tomasi, B. Mennucci, R. Cammi, *Chem. Rev.* **2005**, *105*, 2999-3094. b) M. Cossi, G. Scalmani, N. Rega, V. Barone, *J. Chem. Phys.* **2002**, *117*, 43-54.

View Article Online
DOI: 10.1039/C4DT03174A

Graphical Abstract

The EPR spectrum of a solution of [VO(acac)(BIAN)]Cl containing tbhp and *cis*-cyclooctene shows the presence of a V(IV) species, suggesting its involvement in the catalytic oxidation of alkenes.